Available online at www.sciencedirect.com

Manufacturing Letters

Manufacturing Letters 00 (2023) 000–000

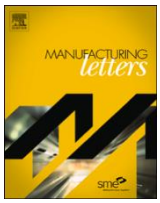

51st SME North American Manufacturing Research Conference (NAMRC 51, 2023)

The Effects of Scratching Speed in Ultrasonic Vibration-Assisted Single Diamond Scratching Process

Yunze Li[a], Muhammad Garbie[a], Yingbin Hu[b], Weilong Cong[a,*]

[a]*Department of Industrial, Manufacturing, and Systems Engineering, Texas Tech University, Lubbock, TX 79409, USA*
[b]*Mechanical and Manufacturing Engineering Department, Miami University, Oxford, OH 45056, USA*

* Corresponding author. Tel.: +1-806-834-6178. *E-mail address:* weilong.cong@ttu.edu

Abstract

Ultrasonic vibration-assisted machining has been widely used in manufacturing hard and brittle materials. Previous studies have shown that the vertical ultrasonic vibration in ultrasound-assisted single diamond scratching can affect the scratching forces, surface quality, and material removal mechanism by two mechanisms: changing the contact mode between the single diamond and the workpiece and increasing the speed of the single diamond relative to the workpiece. However, some studies point out that increasing the speed has little effect on the scratching force and material removal mechanism. Therefore, it is necessary to conduct an investigation that takes into account the effects of both scratching velocity and ultrasonic vibration on scratching force, surface quality, and material removal mechanisms. In this study, the single diamond conventional scratching (CS) and ultrasonic vibration-assisted scratching (UAS) experiments have been conducted at different scratching speeds to investigate the material removal mechanism of ultrasonic vibration-assisted machining. The effects of increasing the scratching speed on cutting forces, material removal mechanism, and machined surface quality are investigated. The results show that in both CS and UAS processes with low to medium scratching speeds (<1000 mm/s), increasing the scratching speed leads to more brittle material removal and lower surface quality. At the same time, the scratching speed has almost no effect on the scratching speed force.

Keywords: Ultrasonic vibration; Single diamond scratching; Scratching speed; Material removal mechanism.

1. Introduction

Monocrystalline silicon and silicon-based wafer substrates have been used in a wide variety of applications in the photovoltaic, semiconductor, medical, aerospace, and optical industries [1-5]. The manufacturing process of monocrystalline silicon wafers wraps single crystal growth, grinding of outer wafers, silicon crystal slicing, etching, and polishing. Among them, grinding and slicing are essential processes that affect the surface quality of the wafers and thus directly influence the cost of subsequent processes. However, due to the low fracture toughness of silicon wafers, micro-cracks and chipping are always generated on the surface of silicon wafers. If the thickness of the damage layer caused by grinding and slicing is relatively small, the amount of material removed in the subsequent etching and polishing processes can be reduced, thus reducing costs and increasing efficiency. In recent years, many researchers have investigated and developed non-conventional machining processes for silicon wafers. Commonly used non-conventional machining processes include jet electrolytic drilling and laser-based machining process [1-3]. The limitations of the jet electrolytic drilling method are the difficulty in machining complex contours, high specific power consumption, and high initial equipment costs. The limitations of the laser-based machining process are the formation of heat-affected zones around the laser scanning path, which may change the silicon wafer's crystal structure, reduce the silicon wafer's strength, and cause oxidation of the silicon

wafer. Compared with jet electrolytic drilling and laser-based machining process, the ultrasonic vibration-assisted machining process has the advantages of lower costs, no heat-affected zone, and the ability to combine with traditional machining processes (such as grinding and slicing) [4,5].

Ultrasonic vibration has a frequency higher than 20 kHz, which is much higher than the natural frequency of a machine or manufacturing system. Combining ultrasonic vibration with a conventional machining system will maintain the system's stability. For this reason, ultrasonic vibration assisted-machining methods have been developed and investigated, such as the rotary ultrasonic machining process (RUM). It has been shown that the ultrasound-assisted machining process offers better cutting surface quality, fewer microcracks and chips, lower cutting forces, and less tool wear than conventional machining processes [6-10]. Because of these advantages, the ultrasonic vibration-assist machining process has the potential to machine silicon wafers. However, the cutting tool's surface used in the machining process usually has a large number of diamond abrasive grains. The material is removed during the contact and impact of these abrasive grains with the surface of the silicon wafer. This multi-abrasive material removal process is complex. It is challenging to investigate the effect of factors such as the indentation depth and speed of individual grains on the material removal mechanism and cutting forces. Therefore, the researchers proposed a simplified method to investigate the material removal mechanism and cutting forces, in which the complex multi-abrasive machining process was simplified into a single abrasive scratching process [11-15]. This method allows a more accurate analysis of the transition of the material removal mechanism from ductile removal to brittle removal.

There are many investigations on the single diamond scratch studies on monocrystalline silicon wafers and other brittle materials [13-18]. Existing studies and theoretical models generally considered that scratching speed has little effect on cutting forces. However, the conclusion about the impact of scratching speed on material removal mechanism and surface quality was inconsistent in different studies. Cao et al. reported that scratching speed has little effect on the material removal mechanisms [13]. The contact mode between a single diamond tool and substrate materials and the effects of ultrasonic vibration on the depth of cut, cutting force, and scratching-induced features were also investigated. However, some other studies reported the scratching speed could affect the formation of microcracks and chippings [14,16]. Zhang et al. explored the scratching on silicon wafers at nanoscale indentation depth [14]. When the scratching speed is high, there is no high-pressure phase in the scratch during the initial stage of brittle material removal. The results show that an amorphous layer forms at the very top of the residual scratch, followed by the original lattice below. Alreja et al. investigated the scratching speed on material removal mechanisms [16]. Results showed that the critical depth of cut under low or high scratching speed was higher than that under medium scratching speed (100-300 mm/s).

To better understand the effects of scratching speed and ultrasonic vibration on cutting forces and material removal mechanisms, in this study, silicon wafers were scratched by a single diamond tool at low and medium velocities under conditions with and without ultrasonic vibration. The horizontal and vertical cutting forces during scratching tests were measured, and the images of the scratching-induced surfaces were gathered. Combining the results of scratching forces and the morphologies of scratching-induced surfaces, the effects of scratching speed on material removal mechanisms under different indentation depths were studied and discussed.

2. Experimental method and condition

As shown in Figure 1, the single diamond scratching tests were conducted by a rotary ultrasonic system (Series 10, Sonic-Mill, Albuquerque, NM, USA). The rotary ultrasonic system includes an ultrasonic system, data acquisition system, horizontal feeding system, and coolant system. The ultrasonic vibration power supply in the ultrasonic spindle system was used to provide vertical mechanical vibration at a high frequency of 20 kHz. The ultrasonic spindle transmitted the mechanical vibration to a single diamond tool. A data acquisition system was used to collect scratch force data during the scratching process, which consisted of a Type 9272 dynamometer, a Type 5070 charge amplifier, a Type 5697A A/D converter, and the software of DynoWare (Kistler, Winterthur, Switzerland). The horizontal feeding system included a linear stage with a machine table (Dslide, Newmark, USA), a motion controller (NSC-A1, Newmark, USA), and the QuickMotion software (Newmark), which were used to

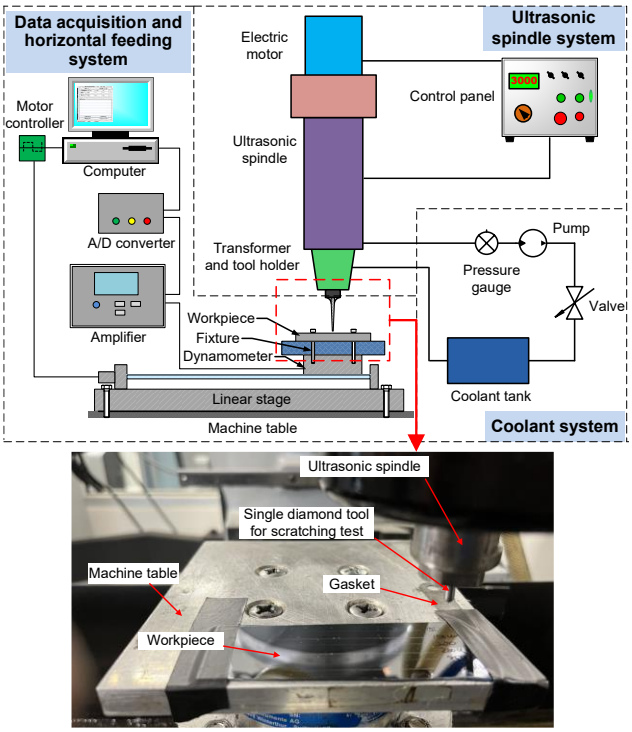

Fig. 1. Experimental setup.

generate the feeding motion. The coolant system consisted of a pump, a coolant tank, and a valve. The cooling system was used

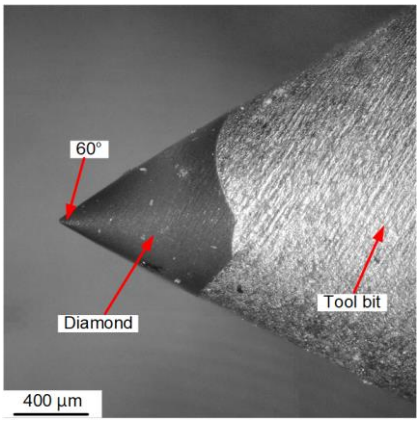

Fig. 2. The single diamond tool in this experiment.

to pump the oil-based coolant around the ultrasonic vibration power supply and ultrasonic spindle to reduce the temperature.

A single diamond tool (Uxcell corp., Hong Kong, China) was fixed on a base to conduct the ultrasonic vibration-assisted scratching (UAS) experiments. As shown in Figure 2, the included angle of the diamond is 60°. The workpiece was a single-side polished round silicon wafer with a thickness of 1000 µm and a diameter of 100 mm (UniversityWafer, Inc.), Massachusetts, USA).

Before the experiments, the silicon wafer was fixed on the machine table with strong adhesive tapes. A gasket raised the right side of the workpiece with a thickness of 20 µm. By changing the position of the machine table, the single diamond tool was moved to the left side of the workpiece and slightly contacted with the workpiece. After that, the linear stage drove the machine table to move at a constant speed to the left. The single diamond tool generated the scratching-induced features with an increasing indentation depth on the workpiece surface. The experimental input parameters are listed in Table 1. The input parameters were selected according to the previously reported investigations. After the scratching tests, the silicon wafers were cleaned with pressure gas. An optical microscope (OM) (DSX-510, OLYMPUS, Tokyo, Japan) was used to obtain the image of scratching-induced features.

3. Kinematic model of single diamond tool

Figure 3 illustrates the trajectory of the single diamond tool in conventional scratching tests (CS) and ultrasonic vibration-assisted scratching tests (UAS). The trajectory of the single diamond tool in CS can be expressed as Equation 1:

$$\begin{cases} x = V_s t \\ y = 0 \\ z = V_s t \cdot \tan(0.12^\circ) \end{cases} \quad (1)$$

Where, Vs is scratching speed, mm/s; t is scratching time, s.

The velocity of the single diamond tool can be expressed as Equation 2:

$$\begin{cases} V(x) = V_s \\ V(y) = 0 \\ V(z) = V_s \cdot \tan(0.12^\circ) \end{cases} \quad (2)$$

The trajectory of the single diamond tool in UAS can be expressed as Equation 3:

$$\begin{cases} x = V_s t \\ y = 0 \\ z = V_s t \cdot \tan(0.12^\circ) + A\sin(2\pi ft) \end{cases} \quad (3)$$

Where, A is the vertical ultrasonic amplitude, mm; f is the vertical ultrasonic frequency, Hz.

The velocity of the single diamond tool in UAS can be expressed as Equation 4:

$$\begin{cases} V(x) = V_s \\ V(y) = 0 \\ V(z) = V_s \cdot \tan(0.12^\circ) + 2\pi fA\cos(2\pi ft) \end{cases} \quad (4)$$

Table 1. Experimental input parameters

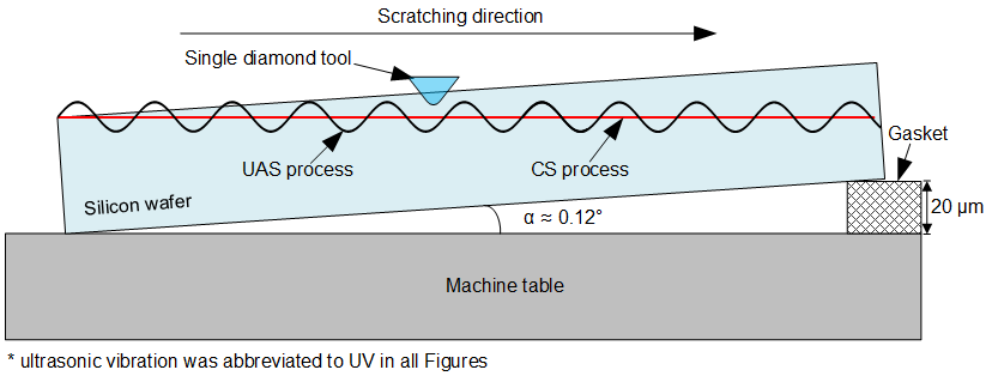

Fig. 3. The illustration of the trajectory of the single diamond tool in the CS and UAS process.

Input fabrication variables	Unit	Values
Scratching speed, V_s	mm/s	50, 150, 250
Vertical ultrasonic amplitude, A	μm	4
Ultrasonic power	%	60

4. Results and discussion

4.1. Effects of scratching speed on scratching force

According to Equation 1, it could be found that during the CS process, the indentation depth was proportional to the scratching time. Therefore, the indentation depth can be calculated from the scratch time and the angle between the silicon wafer and the machine table. Figure 4 (a), Figure 5 (a), and Figure 6 (a) show the curves of indentation depth versus the scratching force in the x-direction and z-direction in the CS process at 50mm/s, 150mm/s, and 250 mm/s scratching speed, respectively. According to Equation 3, the actual indentation depth varies periodically in the UAS process, and its maximum value is more significant than that of CS. To be consistent with the indentation depth in the CS process, the indentation depth in the UAS process in Figure 4 (b), Figure 5 (b), and Figure 6 (b) were the depth without considering the periodic displacement caused by ultrasonic vibration.

As the indentation depth increased in the CS process, the scratching force in the x-direction and z-direction increased continuously. When the scratching speed was 50 mm/s, and the indentation depth increased to 6 μm, the scratching forces in the x-direction and z-direction reached about 0.25 N and 1.5 N, respectively. With the increase of scratching speed to 150 mm/s and 250 mm/s, the average values of the scratching force in the x-direction and z-direction were almost unchanged. However, the magnitude of force variation increased significantly with the increased scratching speed, especially for the force in the x-direction. The fiercer changes in scratching forces usually meant that brittle material removal occurred [17]

In the UAS process, it could be seen that under all levels of scratching speed, the magnitude of force variation in the UAS process was much higher than that in the CS process. According to Equation 4, it can be found that the ultrasonic vibration causes a periodic change in the velocity in the z-direction. The acceleration of a single diamond tool in the UAS process can be expressed as Equation 5:

$$\begin{cases} a(x) = 0 \\ a(y) = 0 \\ a(z) = -4\pi^2 f^2 A \sin(2\pi f t) \end{cases} \tag{5}$$

The maximum value of acceleration during the UAS process is 31582 m^2/s. The large acceleration induced by ultrasonic vibration caused the single diamond tool to strike the surface of the workpiece with significant kinetic energy. The interaction between the single diamond tool and the workpiece caused a drastic change in the scratching force [19].

It could also be seen that the scratching forces in the x-direction and z-direction were increased continuously as the indentation depth increased. When the scratching speed was 50 mm/s, and the indentation depth was 6 μm, the scratching forces in the x-direction and z-direction reached about 0.15 N and 0.5 N, respectively, which were lower than the scratching forces in the CS process. When the scratching speed increased to 150 mm/s and 250 mm/s, the scratching forces in the x-direction and z-direction were similar to those under 50 mm/s

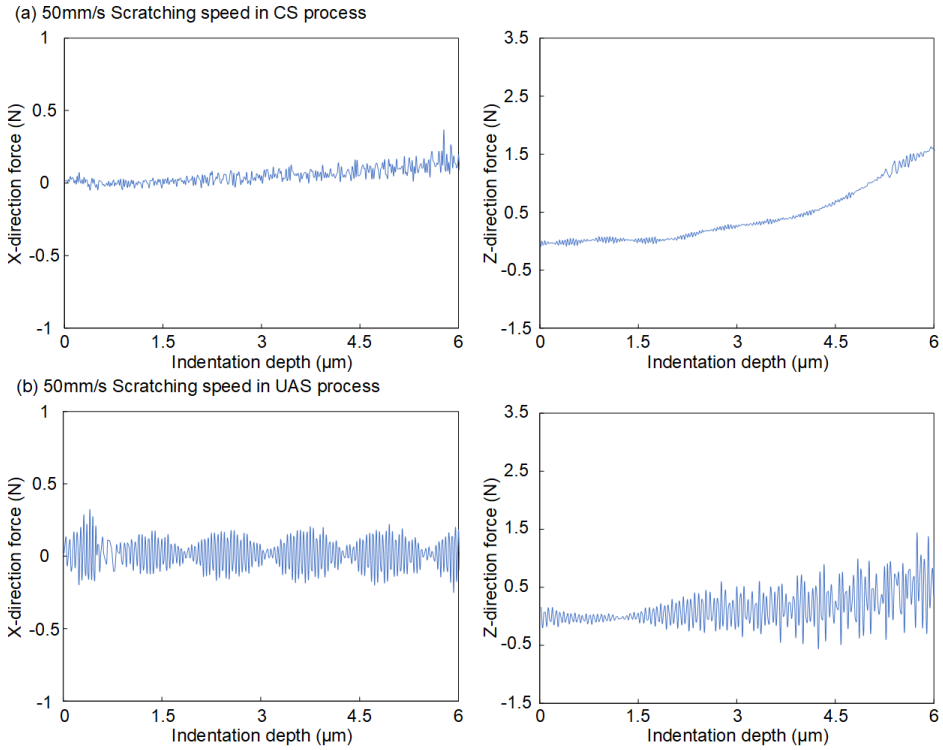

Fig. 4. the curves of indentation depth versus scratching force in the x-direction and z-direction at 50 mm/s scratching speed in (a) CS process and (b) UAS process.

scratching speed. Compared with Equation 2 and Equation 4, it can be found that ultrasonic vibration could result in intermittent contact mode. The impact between a single diamond tool and a workpiece could increase the material removal efficiency and reduce the scratching force [20].

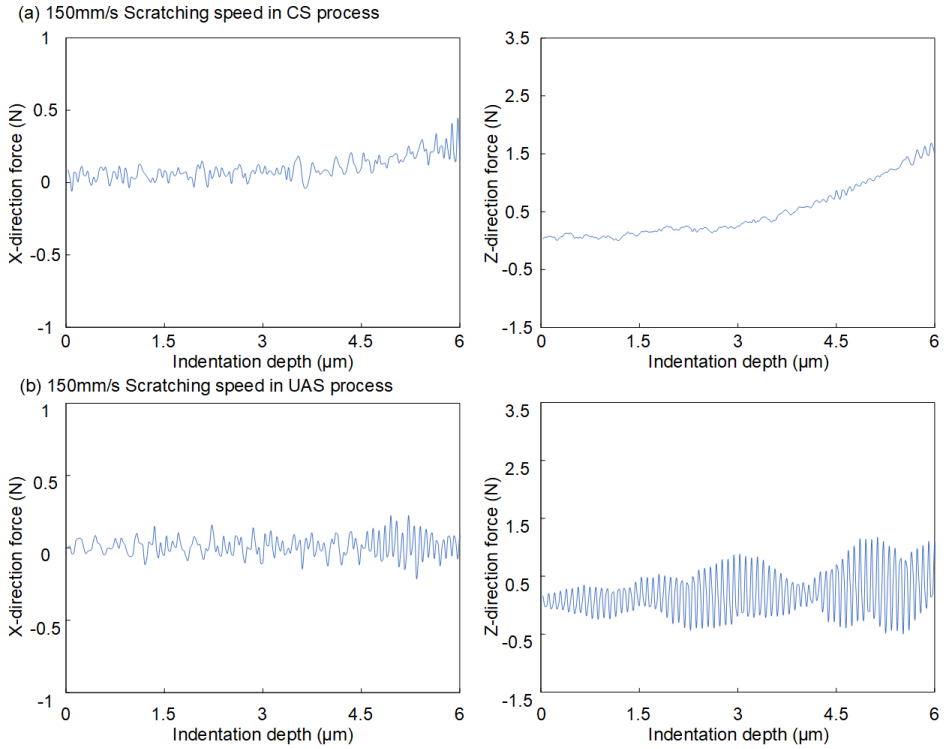

Fig. 5. The curves of indentation depth versus scratching force in the x-direction and z-direction at 150 mm/s scratching speed in (a) CS process and (b) UAS process.

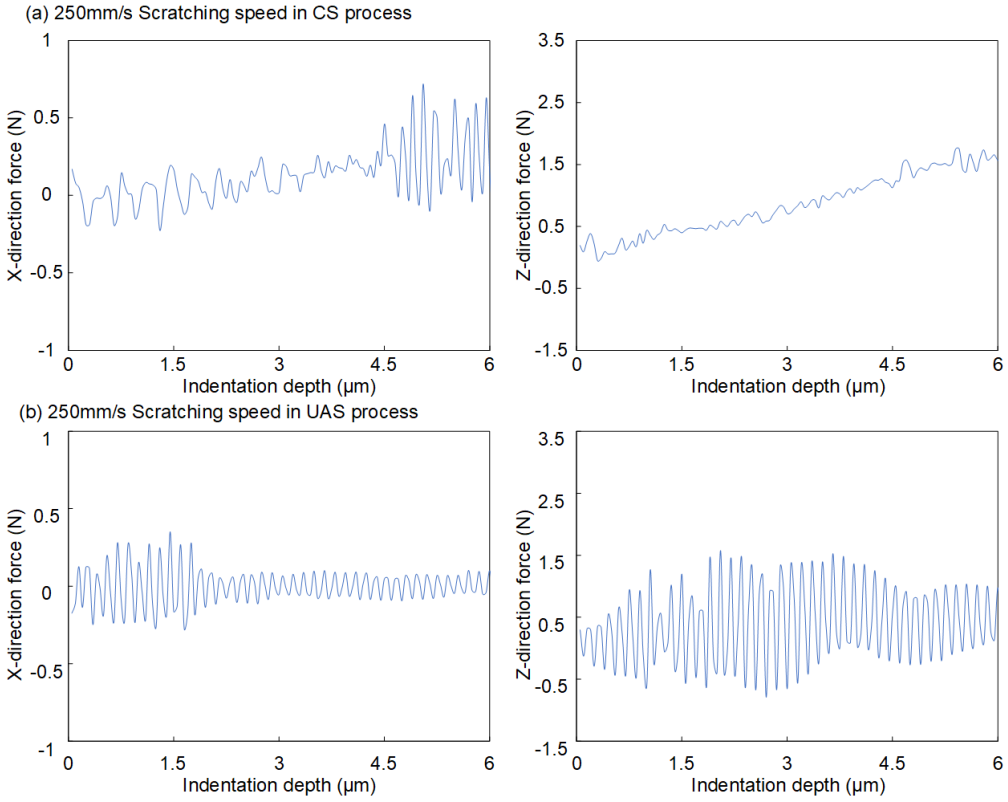

Fig. 6. The curves of indentation depth versus scratching force in the x-direction and z-direction at 250 mm/s scratching speed in (a) CS process and (b) UAS process.

4.2. Effects of scratching speed on surface quality and material removal mechanism

Figure 7 shows the morphologies of the scratching-induced features under different scratching speeds in the CS and UAS process. It could be seen that with the increase of indentation depth, the width of the scratching-induced features was increased.

With the increasing of scratching depth, the scratching forces always increased. The larger scratching force could increase the stress inside the workpiece materials, which resulted in the generation of cracks and the removal of large pieces (high brittle portions). By analyzing the changes in the morphology of scratching-induced features, the occurrence of plastic-brittle material removal transition can be determined. When the scratching-induced features were smooth grooves, there was only plastic material removal. In contrast, when there were cracks and high brittle portions in the scratching-induced features, the brittle material removal occurred. In addition, the magnitudes in scratch force could also be used to determine the material removal mechanism. The smaller magnitudes in the scratch force implied plastic material removal, while the larger magnitudes in the scratch force usually implied the occurrence of brittle material removal [18]. As shown in Figure 7, in the

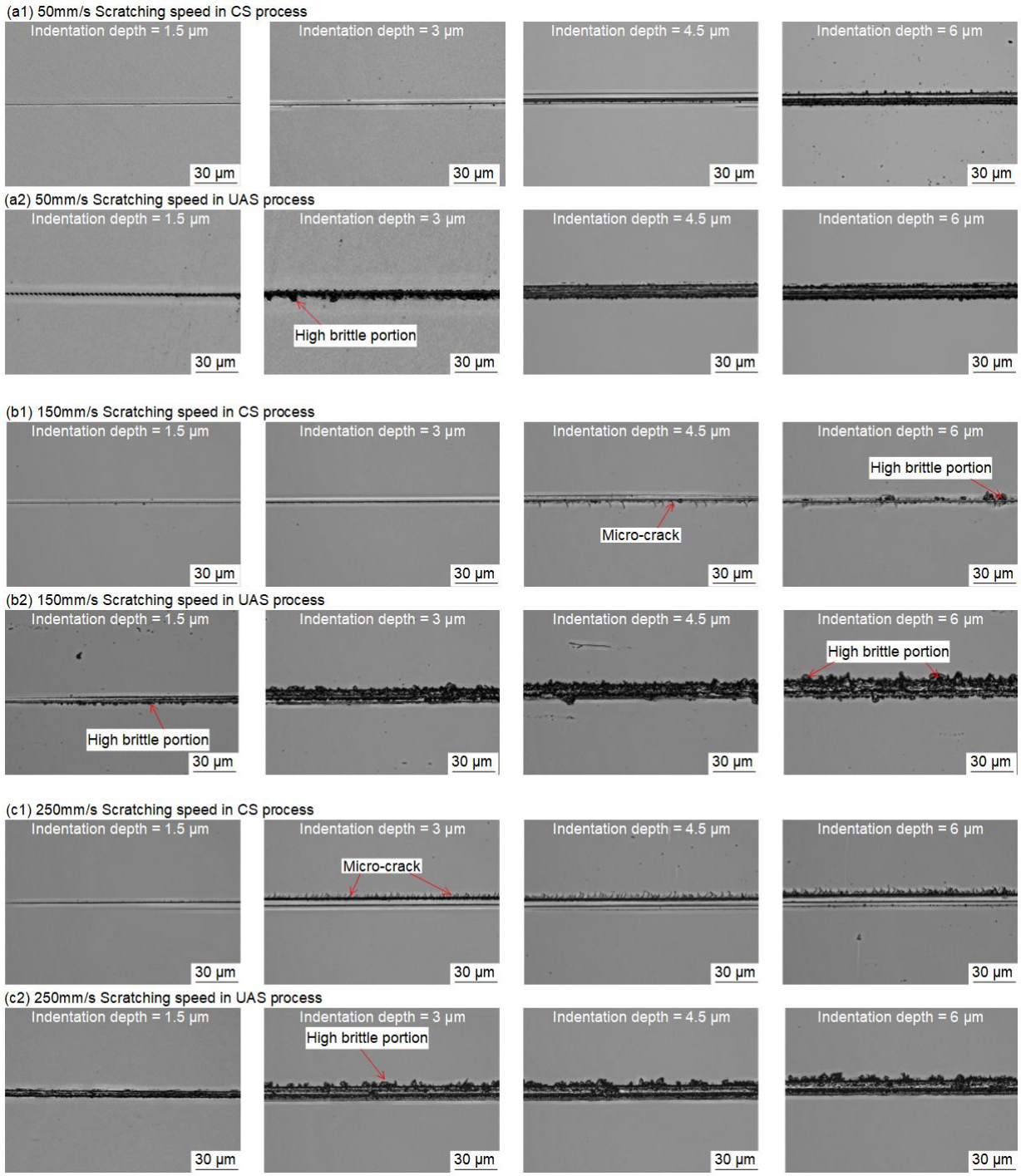

Fig. 7. The morphologies of the scratching-induced features under different scratching speeds in the CS and UAS process.

CS process, the scratching-induced feature was a straight groove, and the material removal mechanisms changed from ductile material removal to brittle material removal as the indentation depth increased. At a low scratching speed of 50mm/s, the scratching-induced features were smooth when the indentation depth was less than 3 μm, which indicated that there was only ductile material removal occurred. When the indentation depth increased to 4.5 μm, high brittle portions were generated around the scratching-induced features, which indicated that the ductile transition to brittle material removal occurred. As the indentation depth further increased to 6 μm, there were more high brittle portions. In addition, As shown in Figure 4(a), Figure 5(a), and Figure 6(a), the magnitude of the scratching forces became larger when the scratching depth increased to 6 μm. The larger number of high brittle portions and larger magnitude of the scratching forces indicated that more materials were removed by the brittle material removal mechanism. When the scratching speed increased to 150 mm/s, brittle material removal also occurred at an indentation depth of 4.5 μm. Compared to the scratching speed of 50 mm/s, a higher scratching speed resulted in more microcracks, and high brittle portions caused by brittle material removal. When the scratching speed further increased to 250 mm/s, the ductile transition to brittle material removal occurred at a smaller indentation depth of 3 μm. The number of microcracks and high brittle portions was further increased. The results showed that a lower scratching speed seemed to inhibit the occurrence of brittle material removal in the CS process.

In the UAS process, the scratching-induced feature had two different modes. When the indentation depth was lower than the ultrasonic vibration amplitude, the scratching-induced feature was in intermittent mode. When the indentation depth was greater than the ultrasonic vibration amplitude, the scratching-induced feature was in continuous mode. At a low scratching speed of 50mm/s, ultrasonic vibration has almost no effect on suppressing the generation of microcracks and high brittle portions. The scratching-induced feature was a smooth and straight groove. However, when the scratching speed was increased to 150 mm/s and 250 mm/s, the UAS process with ultrasonic vibration caused more high brittle portions compared to the CS process. At the same time, the ultrasonic vibration could suppress the generation of microcracks. It also should be noted that although the scratching-induced features in UAS were not as smooth as those in the CS process, we cannot conclude that ultrasonic vibration degraded the surface quality. The reason for this was that vertical ultrasonic vibration could result in a greater actual indentation depth and additional material removal. Comparing the scratching-induced features of UAS with those of CS, the actual scratching width at 3 μm indentation depth in the UAS process was much higher than that in the CS process, which was almost the same as those in the CS process at 6μm indentation depth. Comparing the scratching-induced features in UAS at 3 μm indentation depth and in CS at 6μm indentation depth, it could be found that ultrasonic vibration still helped to suppress the occurrence of brittle material removal and improve the surface quality.

5. Research limitations and future work

This study investigated the effects of scratching speed on the cutting forces and surface quality of CS and UAS processes under low to medium speeds. However, some studies showed that when the scratching speed was further increased to a high level (more than 1000 mm/s), higher speeds could improve the cutting quality [21]. In the future, the authors will build experimental systems that can provide higher scratching speeds. A comprehensive study on the effect of scratching speed on the quality of ultrasonically assisted machining of brittle materials will be conducted.

6. Conclusion

This paper investigated the effects of scratching speed on cutting forces, surface quality, and material removal mechanisms in CS and UAS processes at low to medium speeds. The main conclusions were as follows:

1. In both CS and UAS processes, the increase in the scratching depth resulted in the larger average values of scratching force. However, scratching speed had little effect on the average values of scratching force. In the CS process, the increase in scratching speed could increase the magnitude of the scratching force in the x-direction. In the UAS process, the increase in scratching speed had little effect on the magnitude of the scratching force.

2. Under each level of scratching speed, the magnitude of the scratching force in the UAS process was much higher than that in the CS process due to the interaction between the single diamond tool and the workpiece caused by ultrasonic vibration.

3. In the CS process, increasing the scratching speed led to a decrease in the indentation depth where the transition from ductile to brittle material removal occurred. In addition, at the same indentation depth, the higher scratching speed led to an increase in microcracks and highly brittle portions. In the UAS process, the higher scratching speed could also promote the occurrence of brittle material removal.

4. When the indentation depth was the same, the actual scratching depth and width in the UAS process were higher than that in the CS process. When the actual scratching depth and width were similar (3 μm indentation depth in UAS and 6 μm indentation depth in CS), the surface quality in the UAS process was better than that in the CS process.

Acknowledgments

The work was supported by U.S. National Science Foundation through the award CMMI-2102181.

References

[1] Park, D.-S., Cho, M.-W., Lee, H., & Cho, W.-S. (2004). Micro-grooving of glass using micro-abrasive jet machining. *Journal of Materials Processing Technology, 146*(2), 234-240.

[2] Gurrappa, I., & Binder, L. (2008). Electrodeposition of nanostructured coatings and their characterization—a review. *Science Technology of Advanced Materials*.

[3] Amer, M. S., El-Ashry, M., Dosser, L. R., Hix, K., Maguire, J. F., & Irwin, B. (2005). Femtosecond versus nanosecond laser machining: comparison of induced stresses and structural changes in silicon wafers. *Applied Surface Science, 242*(1-2), 162-167.

[4] Thoe, T., Aspinwall, D., & Wise, M. (1998). Review on ultrasonic machining. *International Journal of Machine Tools Manufacture, 38*(4), 239-255.

[5] Ya, G., Qin, H., Yang, S., & Xu, Y. (2002). Analysis of the rotary ultrasonic machining mechanism. *Journal of Materials Processing Technology, 129*(1-3), 182-185.

[6] Singh, R. P., & Singhal, S. (2017). Investigation of machining characteristics in rotary ultrasonic machining of alumina ceramic. *Materials manufacturing processes, 32*(3), 309-326.
[7] Singh, R. P., & Singhal, S. (2017). Rotary ultrasonic machining of macor ceramic: an experimental investigation and microstructure analysis. *Materials manufacturing processes, 32*(9), 927-939.
[8] Singh, R. P., & Singhal, S. (2018). An experimental study on rotary ultrasonic machining of macor ceramic. *Proceedings of the Institution of Mechanical Engineers, Part B: Journal of Engineering Manufacture, 232*(7), 1221-1234.
[9] Singh, R. P., & Singhal, S. (2018). Experimental study on rotary ultrasonic machining of alumina ceramic: microstructure analysis and multi-response optimization. *Proceedings of the Institution of Mechanical Engineers, Part L: Journal of Materials: Design Applications, 232*(12), 967-986.
[10] Singh, M., Singh, S., & Kumar, S. (2020). Experimental investigation for generation of micro-holes on silicon wafer using electrochemical discharge machining process. *Silicon, 12*(7), 1683-1689.
[11] Gogotsi, Y., Zhou, G., Ku, S.-S., & Cetinkunt, S. (2001). Raman microspectroscopy analysis of pressure-induced metallization in scratching of silicon. *Semiconductor Science Technology, 16*(5), 345.
[12] Zhang, C., Feng, P., & Zhang, J. (2013). Ultrasonic vibration-assisted scratch-induced characteristics of C-plane sapphire with a spherical indenter. *International Journal of Machine Tools Manufacture, 64*, 38-48.
[13] Cao, J., Wu, Y., Lu, D., Fujimoto, M., & Nomura, M. (2014). Material removal behavior in ultrasonic-assisted scratching of SiC ceramics with a single diamond tool. *International Journal of Machine Tools Manufacture, 79*, 49-61.
[14] Zhang, Z., Guo, D., Wang, B., Kang, R., & Zhang, B. (2015). A novel approach of high speed scratching on silicon wafers at nanoscale depths of cut. *Scientific reports, 5*(1), 1-9.
[15] Wallburg, F., Kuna, M., Budnitzki, M., & Schoenfelder, S. (2020). Experimental and numerical analysis of scratching induced damage during diamond wire sawing of silicon. *Wear, 454*, 203328.
[16] Alreja, C., & Subbiah, S. (2019). A study of scratch speed effects on ductile–brittle transition in silicon. *Journal of Micro Nano-Manufacturing, 7*(2).
[17] Ge, M., Zhu, H., Huang, C., Liu, A., & Bi, W. (2018). Investigation on critical crack-free cutting depth for single crystal silicon slicing with fixed abrasive wire saw based on the scratching machining experiments. *Materials Science in Semiconductor Processing, 74*, 261-266.
[18] Liang, Z., Wang, X., Wu, Y., Xie, L., Jiao, L., & Zhao, W. (2013). Experimental study on brittle–ductile transition in elliptical ultrasonic assisted grinding (EUAG) of monocrystal sapphire using single diamond abrasive grain. *International Journal of Machine Tools Manufacture, 71*, 41-51.
[19] Asmael, M., Safaei, B., Zeeshan, Q., Zargar, O., & Nuhu, A. A. (2021). Ultrasonic machining of carbon fiber–reinforced plastic composites: a review. *The International Journal of Advanced Manufacturing Technology, 113*(11), 3079-3120.
[20] Komaraiah, M., & Narasimha Reddy, P. (1991). Rotary ultrasonic machining—a new cutting process and its performance. *International Journal of Production Research, 29*(11), 2177-2187.
[21] Mukaiyama, K., Ozaki, M., & Wada, T. (2017). Study on ductile-brittle transition of single crystal silicon by a scratching test using a single diamond tool. In *2017 8th International Conference on Mechanical and Aerospace Engineering (ICMAE)*, (pp.40-44). IEEE.